

# Study on the measurement of isoprene by Differential Optical Absorption Spectroscopy

Song Gao<sup>1,4</sup>, Shanshan Wang<sup>1,2</sup>, Chuanqi Gu<sup>1</sup>, Jian Zhu<sup>1</sup>, Ruifeng Zhang<sup>1</sup>, Yanlin Guo<sup>1</sup>, Yuhao Yan<sup>1</sup>, Binzhou<sup>1,2,3,5</sup>

<sup>1</sup>Department example, University example, city, postal code, country Shanghai Key Laboratory of Atmospheric Particle Pollution and Prevention (LAP<sup>3</sup>), Department of Environmental Science and Engineering, Fudan University, Shanghai 200438, China

<sup>2</sup>Institute of Eco-Chongming (IEC), No. 20 Cuinia Road, Shanghai 202162, China

<sup>3</sup>Zhuhai Fudan Innovation Institute, Zhuhai, 519000, China

<sup>4</sup>Shanghai Environmental Monitoring Center, Shanghai, 200235, China

<sup>5</sup>Institute of Atmospheric Sciences, Fudan University, Shanghai, 200433, China

*Correspondence to:* Shanshan Wang (shanshanwang@fudan.edu.cn) and Bin Zhou (binzhou@fudan.edu.cn)

**Abstract.** In this paper, the continuous on-line measurements of isoprene in the atmosphere have been carried out by using the Differential Optical Absorption Spectroscopy (DOAS) in the band of 202.71-227.72 nm for the first time. Under the zero optical path in the laboratory, different equivalent concentrations of isoprene were measured by the combination of known concentration gas and series calibration cells. The correlation between the measured concentrations and the equivalent concentrations was 0.9995, and the slope was 1.065. The correlation coefficient between DOAS and on-line VOCs instrument observed from 23 days field observation is 0.85 with a slope of 0.86. It is estimated that the detection limit of isoprene with DOAS is about 0.1 ppb at an optical path of 75 m, and it is verified that isoprene could be measured in the ultraviolet absorption band using DOAS method with high temporal resolution and low maintenance cost.

## 1. Introduction

Isoprene, named as 2-methyl-1,3-butadiene (C<sub>5</sub>H<sub>8</sub>), is an important BVOCs (Biogenic Volatile Organic Compounds) in the atmosphere. Its global emission rate is about 500 TgCyr<sup>-1</sup> (Sindelarova et al., 2014). Isoprene accounts for 70% of global BVOCs emissions (Aydin et al., 2014). Land vegetation and other natural sources contribute 90% of isoprene in the atmosphere (Zhang et al., 2016), and anthropogenic emissions mainly come from industrial activities. Isoprene, as a typical pentadiene hydrocarbon, has a higher activity than that of ordinary anthropogenic VOCs (Lian et al., 2020), and its lifetime in the boundary layer is only about half an hour (Zheng et al., 2015). Due to high volatility and reaction activity, isoprene can accelerate the reaction between atmospheric substances, and it is easy to react with strong oxidizing substances (OH, NO<sub>3</sub> radicals, etc.), and also affects the balance between NO<sub>x</sub> (NO<sub>x</sub> = NO + NO<sub>2</sub>) and O<sub>3</sub> in the atmosphere. Isoprene is also the precursor of secondary organic aerosol (SOA) (Zeng et al., 2018).

Isoprene produced by plants is a byproduct of photosynthesis, its emission intensity directly relates to the abundance of plants, leaf area index, and plant species. Meteorological parameters, such as temperature, radiation intensity and humidity, can also affect the emission of isoprene (Bai, 2015). In the daytime, the chemical process oxidized by OH is the main sink of isoprene. Due to the existence of multiple double bonds, the additional reaction with OH will lead to the formation of a variety of products and the formation of RO<sub>2</sub>. In the presence of NO<sub>x</sub>, RO<sub>2</sub> can be further reacted to convert RO and HO<sub>2</sub>, causing the mutual conversion of free radicals and the accumulation of ozone, which affects the balance of O<sub>3</sub> in the atmosphere (Chen et

38 al., 2020; Lu et al., 2018; Zhu et al., 2020). Meanwhile, the reaction of isoprene with NO<sub>3</sub> mainly occurs at night. Although the  
 39 reaction only accounts for 6%-7% of the total isoprene oxidation, it is an important way to remove NO<sub>3</sub> (Xie et al., 2013).

40  
 41 In recent years, with the increase of urban vegetation diversity, the emission intensity of urban BVOCs has a significant  
 42 upward trend. The monitoring and control of isoprene in urban ecosystem has also attracted more and more attention. Because  
 43 isoprene concentration in the atmosphere is low, and the life time is short, high precision and accuracy methods are needed for  
 44 monitoring. Currently, general methods, including gas chromatography-mass spectrometry (GC-MS), proton transfer reaction  
 45 mass spectrometry (PTR-MS), and chemical ionization mass spectrometry (CIMS) et al. were introduced to measure isoprene.

46  
 47 GC-MS utilizes the high separation ability of gas chromatography to separate the components of environmental samples, and  
 48 then measures the different compounds with the mass spectrometer. With the advantages of high precision and stability,  
 49 GC-MS can distinguish most VOCs qualitatively and quantitatively, however, is difficult in maintaining and operating due to  
 50 the complex requirements in power, temperature control, and special carrier gas. GC-MS measurement generally requires  
 51 sampling, preservation, and pre-treatment before analysis. During this process, the sample may change to some extent,  
 52 resulting in inaccurate results.

53  
 54 PTR-MS is the chemical ionization of gas sample through proton transfer in drift tube. The proton source is usually H<sub>3</sub>O<sup>+</sup>. The  
 55 fixed length of the drift tube provides a fixed reaction time for the ions as they move along the drift tube. The sample air is  
 56 continuously pumped through the drift tube and the VOCs in the sample react with H<sub>3</sub>O<sup>+</sup> to be ionized, and then enter the mass  
 57 spectrometer to be detected. The disadvantage of PTR-MS is that it completely relies on mass spectrometry to provide the  
 58 identification of mixtures. VOCs as a class of substances, it is possible to have the same molecular weight or the same mass of  
 59 fragment ions and parent ions. In this case, it is difficult to determine all species present and their respective concentrations. A  
 60 solution to this is to combine GC with PTR-MS (Robert et al., 2009).

61  
 62 CIMS (Leibrock & Huey, 2000) retains the qualitative ability of mass spectrometry, and coupling the traditional air sampler  
 63 with mass spectrometry technology. However, this method is not sensitive to low concentration isoprene. In addition, the VOC  
 64 composition in the atmosphere is complex, and the unknown composition may react with benzene reagent to interfere with the  
 65 measurement results. Table 1 lists the comparison of performance of these three methods for isoprene measurements together  
 66 with DOAS method in this study.

67  
 68 **Table 1. Comparison of different on-line methods for isoprene measurement.**

|  | DOAS<br>(this study)                               | GC-MS<br>(Gong et al., 2018)                 | PTR-MS<br>(Eerdekens et al., 2009) | CIMS<br>(Leibrock et al.,<br>2003)       |
|--|--|--|------------------------------------|--|
| Time resolution                            | 1 min  | 30-60 min                                    | 0.5-2 min                          | 1.65 s                                   |
| Accuracy<br>(Correlation with<br>GC-MS/GC) | R=0.85   | R>0.99<br>(with offline)                     | 0.95                               | R=0.78                                   |
| Detection Limit                            | 10 ppt   | 4 ppt  | 100 ppt                            | <30 ppt                                  |
| Platform                                   | Stationary<br>/ conditional<br>mobile              | Stationary<br>/ mobile                       | Stationary<br>/ mobile             | Stationary<br>/ mobile                   |
| Advantages                                 | No sampling<br>Easy operation<br>Simple instrument | High precision<br>Accurate<br>quantification | Fast responses<br>High precision   | High time resolution<br>Good sensitivity |

|               |   |   |  |  |
|---------------|---|---|--|--|
| Disadvantages | Impacts by weather conditions<br>Impacts of interferences | Time consuming<br>Calibration needed<br>Difficult operating and maintaining | Molecule or fragment ion of the same mass cannot be differentiated | Interference of unidentified components<br>Expensive equipment |
|---------------|---|---|--|--|

69

70 In addition, a portable gas chromatograph (iDirac) equipped with photo-ionization detector to measure isoprene was proposed  
71 by Conor et al. (2020) in Cambridge University. The instrument is an improved technology for GC-MS, which can work  
72 independently weeks to months in the field environment. Previous studies rarely mentioned the measurement of isoprene by  
73 spectral method. Brauer et al. (2014) measured the infrared spectrum of isoprene by Fourier transform spectrometer, and found  
74 that isoprene has a strong absorption near 11000 nm, which provides a new possibility for the measurement of isoprene by  
75 spectral technology. So far, however, few people have mentioned the measurement of isoprene by ultraviolet spectroscope. In  
76 this paper, an on-line measurement method with high temporal resolution for isoprene in the atmosphere is proposed by using  
77 the DOAS technology in the far ultraviolet band.

## 78 2. Measurement method

### 79 2.1 Instrument introduction and spectral analysis

80 DOAS technology was proposed by Platt et al. (1979, 1980) in 1970s for the first time. The principle of the instrument was  
81 detailed in other literature (Platt & Stutz, 2008), here is the description of deep UV-DOAS. The system is mainly composed  
82 of light source, transmitting telescope, receiving telescope, spectroscope, and computer, etc. (see Figure 2). The transmitting  
83 and receiving telescopes are located at both ends of the measuring optical path with a distance of 75 m. Since the  
84 measurement of isoprene is in deep ultraviolet, we choose deuterium lamp (L6311-50, Hamamatsu, 35 W) as light source.  
85 The aperture of the transmitting telescope is 76 mm, with a UV enhanced spherical mirror with a focal length of 304 mm.  
86 The aperture of the receiving telescope is 152 mm with a UV enhanced spherical mirror with a focal length of 608 mm. A  
87 spectroscope (B&W TEK Inc. BRC741E-1024) with a spectral range of 185-400 nm, a spectral resolution of 0.75 nm  
88 FWHM (Full Width Half Maximum), and a 1024-pixel photodiode array was used as detector to record the spectrum. The  
89 measurement routine is that the light emitted by the light source is collimated by the transmitting telescope and then sent out,  
90 after a certain distance of transmission, it is collected by the receiving telescope and focused on the incident end of the  
91 optical fiber. The optical fiber feeds the light into the spectroscope, which detects the light signal and sends it to the  
92 computer for spectral analysis.

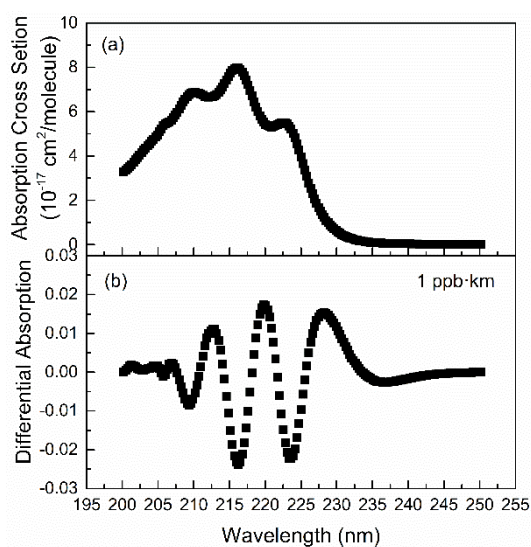
93

94 The measured atmospheric spectrum contains the absorption information of molecules in the atmosphere. After removing the  
95 Rayleigh scattering and Mie scattering, as well as the broadband absorption of molecules by high pass filtering, the so-called  
96 differential absorption spectrum is obtained. This high pass filtering is performed by a high pass binomial on the spectrum  
97 using the iterations of 500 twice aiming to eliminate the broadband structures. The concentration of the corresponding  
98 atmospheric components can be retrieved by fitting the differential absorption spectrum with the differential absorption cross  
99 section of the measured molecules. The reference spectrum during laboratory experiments was recorded by receiving the  
100 light beam close the transmitting device, suggesting the zero light path and none absorption of isoprene. In the field  
101 measurements, the measured atmospheric spectrum collected at 00:00 LT on July 1, 2018 was used as the reference spectrum  
102 considering it is “clean” without isoprene absorption.

103

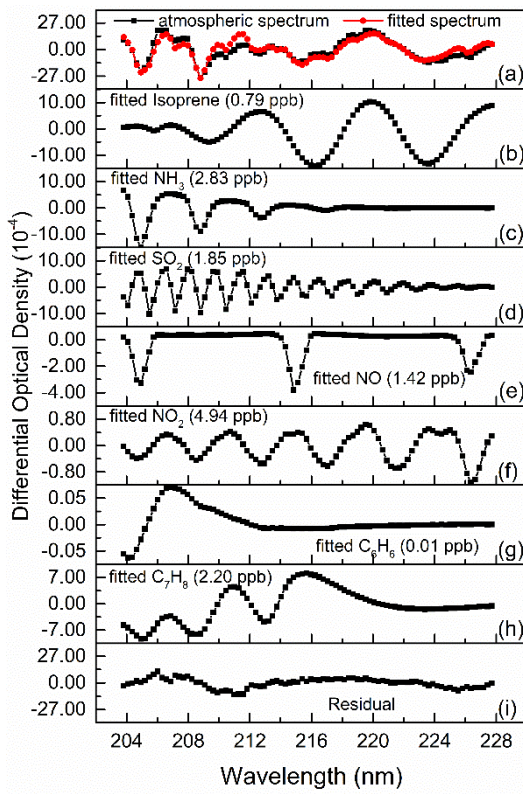
104 Isoprene has strong absorptions between 200.0-225.0 nm, among which there are relatively obvious absorption peaks  
105 (Martins et al., 2009) near 210.0 nm, 216.0 nm and 222.1 nm, as shown in Figure 1(a). After high pass filtering, the

106 differential absorption spectrum (1 ppb\*km) of isoprene is shown in Figure 1(b). According to its differential absorption  
107 characteristics, the fitting band of isoprene is 202.71-227.72 nm. Within this band, there are also absorptions of NH<sub>3</sub> (Chen et  
108 al., 1999), SO<sub>2</sub> (Wu et al., 2000), NO, NO<sub>2</sub> (Mérieulle et al., 1995), C<sub>6</sub>H<sub>6</sub> (Dawes et al., 2017), C<sub>7</sub>H<sub>8</sub> (Serralheiro et al., 2015),  
109 etc. These high-resolution absorption cross sections are convoluted with the instrumental wavelength before introducing into  
110 the spectral fitting. The absorption of NO used here was measured in laboratory with known concentration gas by using the  
111 same instrument. Therefore, the absorption of these components is also considered in the process of spectral retrieving.  
112 Figure 2 displays an example of the spectral fitting of an actual atmospheric spectrum (measured at 2018-07-08 12: 47). In  
113 Fig.2 (a), the black line is the measured spectrum and the red line is the fitting spectrum (0.79 ppb isoprene, 2.83 ppb NH<sub>3</sub>,  
114 1.85 ppb SO<sub>2</sub>, 1.42 ppb NO, 4.94 ppb NO<sub>2</sub>, 0.01 ppb C<sub>6</sub>H<sub>6</sub>, 2.20 ppb C<sub>7</sub>H<sub>8</sub>), while the fitting residual (standard deviation is  
115 4.76E-4) is shown in Fig. 2(i). The differential optical density of isoprene and other interference trace gases were displayed  
116 in Fig. 2(b) to (h), respectively, of which the measurement error of isoprene is about 10.6% according to the method  
117 proposed by Stutz and Platt (1996).



118

119 Figure 1. The absorption cross-section and differential absorption spectrum of isoprene in 1 ppb\*km, together with other  
120 trace gases with absorptions.



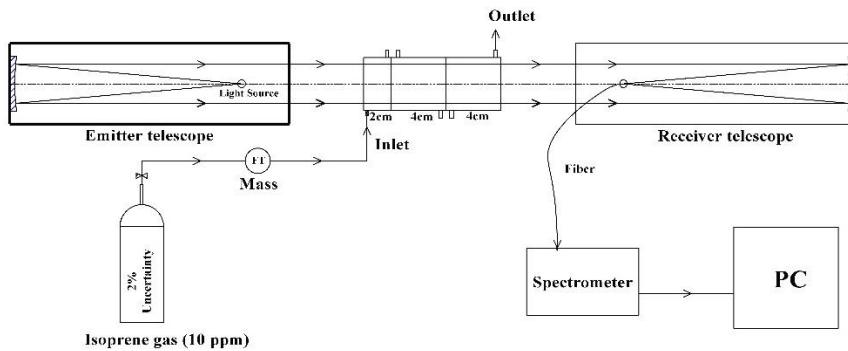
121

122 Figure 2. Example of the spectral fitting of an actual atmospheric spectrum (measured at 2018-07-08 12: 47).

123 **2.2 Calibration experiment**

124 In order to verify the accuracy of measurement results, isoprene gas with known concentration is used to calibrate the  
 125 instrument in the laboratory. The method is to close the emitting telescope and receiving telescope (close to zero optical path)  
 126 in the laboratory, and then a series absorption cell was placed between the telescopes. 10 ppm isoprene gas was injected into  
 127 the cells at a constant flow rate of 100 ml/min, and then the corresponding concentration under different cell combinations  
 128 was measured, as shown in Figure 3.

129



130

131 Figure 3. The scheme of the calibration system

132 The absorption cell group is composed of one 2 cm and two 4 cm long cells in series. When using different combination of  
 133 cells, different equivalent concentrations ( $C_E$ ) (equivalent to the average concentration in the 100 m optical path) can be  
 134 obtained. The specific combination and corresponding equivalent concentrations, as well as the actual measurement  
 135 concentrations ( $C_M$ ) are shown in Table 2.

136 Table 2: the calibration results in different gas cells combination

| Length of cells | $C_E$ (ppb) | $C_M$ (ppb) |
|-----------------|-------------|-------------|
|-----------------|-------------|-------------|

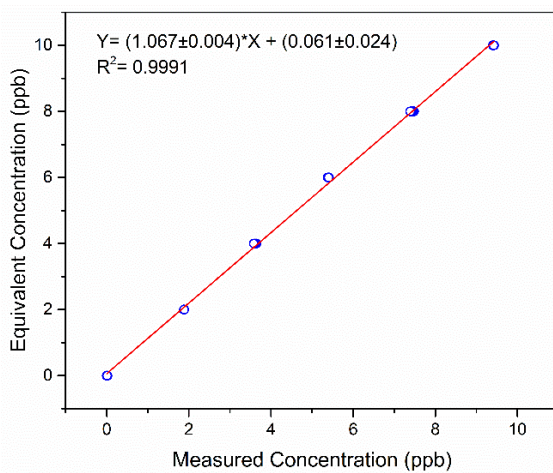
|                    |       |            |
|--------------------|-------|------------|
| empty              | 0     | 0.01±0.005 |
| 2 cm               | 2.00  | 1.88±0.004 |
| 4 cm               | 4.00  | 3.61±0.019 |
| 2 cm + 4 cm        | 6.00  | 5.40±0.009 |
| 4 cm + 4 cm        | 8.00  | 7.44±0.030 |
| 2 cm + 4 cm + 4 cm | 10.00 | 9.42±0.010 |

137

138 Figure 4 shows the linear fit of calibration results. The ordinate in the figure is the equivalent concentration, and the abscissa  
 139 is the measured concentration. For six measuring points including the zero point, the linear fitting correlation coefficient R is  
 140 0.9995. The relationship between the equivalent concentration and the measured concentration is shown in the following  
 141 equation (1). For future measurement results of the actual atmosphere, equation (1) will be used to calibrate the measured  
 142 data.

143

$$C_E = (0.061 \pm 0.024) + (1.067 \pm 0.004) * C_M \quad (1)$$



144

145 Figure 4. The linear fitting of calibration results for isoprene measurement

### 146 3. Field comparison experiment and discussion

#### 147 3.1 Comparison with on-line VOCs results

148 In order to further verify the reliability of the DOAS method in actual atmospheric measurement, in July 2018, the field  
 149 measurement results of the DOAS were compared with the on-line VOCs (TH-300B on-line VOCs monitoring system)  
 150 analyzer (Zhu et al., 2020), which is based on the GC-MS technology. DOAS instrument is installed on the 7th floor of the  
 151 Environmental Science Building (31.344 ° N, 121.518 ° E) in Jiangwan campus of Fudan University, as shown in Figure 4.  
 152 The optical path is about 25 m above the ground. The transmitting telescope is at the west part of the building (A in Figure 5),  
 153 while the receiving telescope is at the east part (B in Figure 5). The distance between the telescopes is 75 m. The on-line  
 154 VOCs instrument is located in Xinjiangwan City monitoring station of Shanghai Environmental Monitoring Center (C in  
 155 Figure 5). The straight-line distance is about 0.5 km to the south of the DOAS instrument. The coverage rate of plants around  
 156 the observation sites is high, mainly including pine, camphor, etc., and a large number of lawns are also distributed.  
 157 Meteorological parameters were recorded by the automatic weather station (CAMS620-HM, Huatron Technology Co. Ltd)  
 158 co-located with the DOAS instrument.

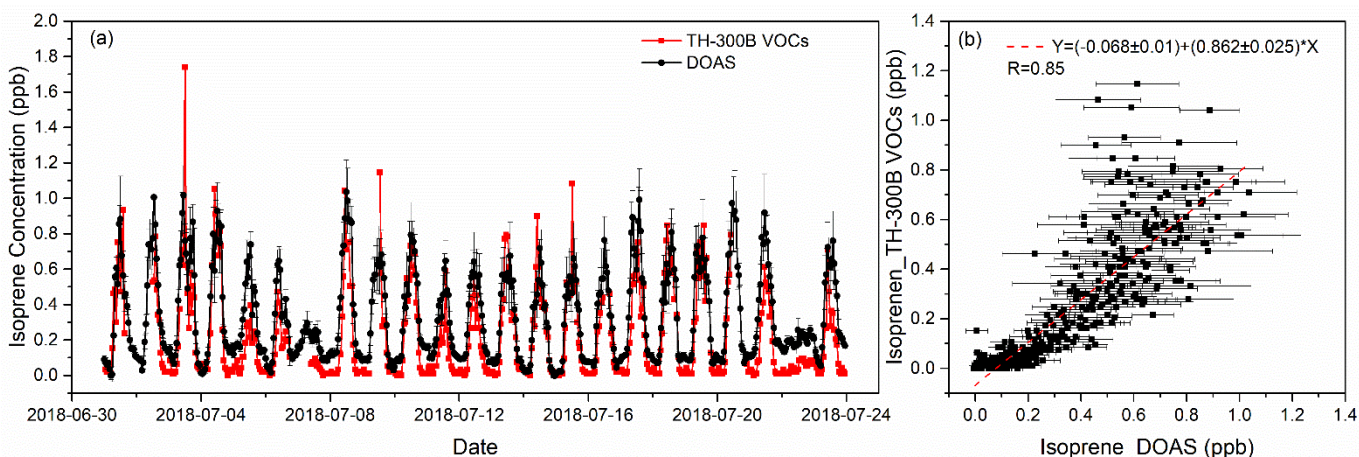
159



160  
 161 Figure 5. Field measurement sites of DOAS and on-line VOCs, A is the transmitting telescope, B is the receiving telescope,  
 162 and C is the on-line VOCs, the yellow arrow is the light path of DOAS. This map is sourced from © Baidu

163  
 164 The comparison experiment was carried out from July 1<sup>st</sup> to 23<sup>rd</sup>, 2018. The temporal resolution of DOAS was 1 min, while  
 165 that of on-line VOCs was 1 h. In order to match the temporal resolution, DOAS data were averaged hourly. Moreover, the  
 166 measured spectra with low light intensity and high integration time were excluded from the spectral fitting and data  
 167 processing, which are mainly due to the unfavorable weather condition influencing the measurements. The spectral were also  
 168 corrected for offset before introducing fitting. Figure 6(a) shows the time series of the isoprene data measured by these two  
 169 instruments, which are in a good agreement. The average values of DOAS and on-line VOCs were 0.325 ppb and 0.217 ppb  
 170 respectively, and the standard deviation (SD) was 0.254 ppb (N=551) and 0.257 ppb (N=466), respectively. The average  
 171 value of DOAS results is higher than that of the on-line VOCs mainly because, at night, DOAS can still detect a certain  
 172 concentration in most cases, most of which are between 0.02-0.10 ppb, while most of on-line VOCs data are between 0-0.05  
 173 ppb. Due to the missing of some data of on-line VOCs during the comparison period, totally 466 sets of hourly data were  
 174 used to analyze the correlation between these two instruments. As shown in Figure 6(b), the correlation coefficient is 0.85  
 175 and the slope is 0.86.

176



177  
 178 Figure 6. The comparison of hourly isoprene measured by DOAS and on-line VOCs during the field measurement

179  
 180 The main reason for the difference of DOAS and on-line VOCs results is that the sampling and measurement heights of the  
 181 two instruments are different. The light path of DOAS is about 25 m above the ground, while the sampling height of on-line  
 182 VOCs instrument is about 10 m. In addition to the 500 m distance between these two sites, the air sampled by VOCs

183 analyzer or penetrated by DOAS light beam are completely different. Considering the inhomogeneity spatial distribution of  
184 isoprene, this will lead to different data results between two instruments. Considering the sampling of on-line VOCs is  
185 through the sampling tube, isoprene will be more or less lost during the sampling process, which could be up to 10% for  
186 some high carbons VOCs (EPA, 2019). In order to ensure the authenticity and accuracy of the observed data, the working  
187 status and response of the TH-300B monitoring system were inspected every day. Daily calibrations were performed  
188 automatically at 00:00 to 01:00 LT. In addition, the external standard method for the FID and the internal standard method  
189 for the MS were adopted. The daily calibration operated at midnight could make the on-line VOCs observed value close to  
190 the zero point, which may deviate from the real abundance. Since the observation is in summer, there is also a very high  
191 temperature at night during the observation period, i.e. 27.1°C (19:00-06:00 next morning). In addition, the release of  
192 isoprene produced by the leaves of plants in the daytime is delayed to some extent, resulting in a certain concentration of  
193 isoprene remaining at night, so that we think the data of DOAS is more reasonable. Those two reasons will eventually lead to  
194 DOAS measurement results higher than online VOCs instruments, especially when the isoprene concentration is very low at  
195 night, the difference is more obvious. On the other hand, the error of DOAS method would also be the possible reason  
196 causing the difference with VOCs analyzer.

197  
198 It can also be seen from Figure 6(b) that when the isoprene concentration is higher than 0.5 ppb, the measurement results of  
199 the two instruments show large scattering. The different measurement principles, especially the difference of sampling time  
200 can also cause the scattering of the results of two instruments. On-line VOCs only has about 50% of the time (1h) to be used  
201 to sampling, while the rest of the time is used for analysis. But DOAS is almost continuous measurement with just a little  
202 part of time to be used for analysis (about 1s per minute), this difference will affect the consistency of results. Meanwhile,  
203 there are various vegetations between the instruments, when the wind direction changes, the emission of this part of  
204 vegetation will also cause the difference between the results of the instruments. But in general, DOAS and on-line VOCs  
205 analyzers show a good agreement in the comparison of mean and correlation of measured data.

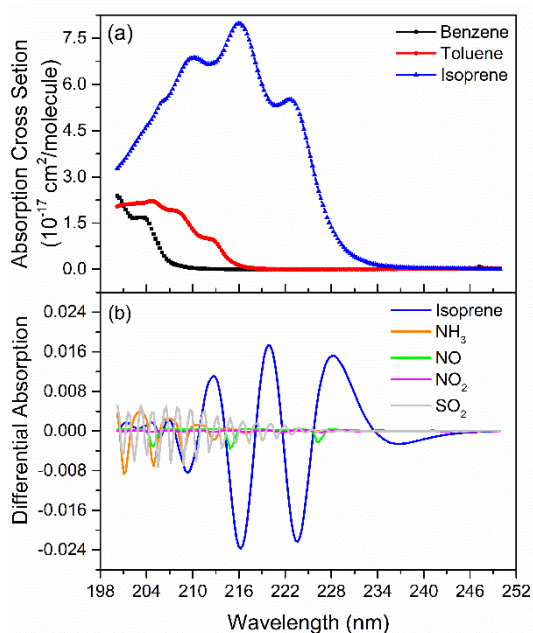
### 206 **3.2 Detection limit evaluation**

207 The detection limit of DOAS mainly depends on the signal-to-noise ratio of the spectrum. Under the condition of zero light  
208 path in the laboratory, the zero noise (standard deviation of the results) of isoprene is 0.005 ppb, the detection limit can be  
209 definite as two times of zero noise, so that the detection limit of the system is 0.010 ppb (HJ 654-2013). However, in the real  
210 atmospheric measurement, it is difficult to determine the actual detection limit due to the varied environment and the  
211 interference of other gases. The detection limit of DOAS in real atmosphere is mainly determined by the residual of spectral  
212 fitting. The residual mainly comes from the absorption of interfering substances, the change of lamp spectral intensity and  
213 structure, the spectral shift caused by the change of ambient temperature of the spectrometer, and the noise of the detector.  
214 Since the stability of light source and spectrometer will influence the fitting residual and instrumental performance,  
215 temperature control was adopted for the spectrometer and operating ambient. In order to reduce the influence of these factors  
216 on the measurement, in the process of spectra fitting, the absorption of interfering substances and the spectral structure of  
217 lamp are necessary to be considered together with the isoprene absorption spectrum. The lamp spectrum will be also  
218 introduced into the fitting process if obvious lamp spectral structure was observed in the residual. At the same time, it is also  
219 necessary to calibrate the spectral drift. However, there are still some residual remain after the spectral fitting due to possible  
220 imperfect reference spectra. Overall, the averaged measurement errors of isoprene were estimated lower than 20%.

221  
222 In the fitting band of isoprene, the absorption of NO, benzene and toluene are the main interference factors. The reason for  
223 the influence of NO is that there are three obvious absorption peaks of NO in the fitting band. After high pass filtering, there  
224 is component in the differential absorption cross section of NO similar to the variation frequency of isoprene's differential



225 absorption spectrum. After the analysis of the measurement results, the impact of NO on isoprene is about 0.3% of its  
226 concentration. But the effect of NO is mainly in the morning and evening rush hour. The influence of benzene and toluene is  
227 mainly due to their strong absorptions in the fitting band of the spectrum. Their presence will lead to a significant reduction  
228 in the spectral intensity in this band, resulting in a reduction in the signal-to-noise ratio of the spectrum. During the  
229 comparison experiment, high concentration of benzene or toluene occasionally occurs, resulting in a large fitting residual.  
230 Other aromatics, such as xylene and styrene, also absorb strongly in the fitting band, but because of their lower concentration  
231 in the natural atmosphere, their impacts on isoprene are significantly smaller than that of benzene and toluene. Although NH<sub>3</sub>,  
232 SO<sub>2</sub> and NO<sub>2</sub> have absorption in the fitting band, their differential absorption variation frequency is significantly higher than  
233 that of isoprene, and only overlaps in parts of fitting band, so that they have little influence on the isoprene measurement. Fig.  
234 7a shows the absorption cross section of benzene, toluene and isoprene, while Fig. 7b illustrates the differential absorption  
235 spectra (1 ppb\*km) of NO, SO<sub>2</sub>, NO<sub>2</sub>, NH<sub>3</sub> and isoprene obtained by applying high filter pass same as the spectral fitting  
236 process. Moreover, the employment of the “clean” atmospheric spectrum, instead of the reference spectrum without any  
237 absorption under zero optical path, also introduces the uncertainty into the spectral fitting, because it may contain few of  
238 isoprene absorption.



239  
240 Figure 7. The absorption cross section of benzene, toluene and isoprene (a), the differential absorption spectra (1 ppb\*km) of  
241 NO, SO<sub>2</sub>, NO<sub>2</sub>, NH<sub>3</sub> and isoprene (b)

242 Whether it is benzene, toluene, or NO, SO<sub>2</sub>, NO<sub>2</sub> and NH<sub>3</sub>, they all exist together with isoprene in the atmosphere. Therefore,  
243 their influences on isoprene measurement are common. In order to ensure the quality of results, the data with a residual of  
244 more than 0.0005 are filtered out. In a total of 33120 sets of data during 23 days observation, 1137 sets are filtered out, and  
245 the valid rate of data is 96.6%. The average residual of all valid data is 0.000234. In order to evaluate the detection limit of  
246 DOAS in the real atmospheric measurement, we made a statistic on 16387 sets of data with the concentration of isoprene  
247 lower than 0.1 ppb (assuming that the isoprene in the atmosphere is close to zero at this time), and the standard deviation is  
248 0.0499 ppb, so the detection limit of DOAS instrument in the field measurement is no more than 0.1 ppb (twice the standard  
249 deviation).

#### 250 4. Conclusion

251 This paper introduces, for the first time, the continuous on-line measurement of isoprene in the atmosphere by means of  
252 DOAS in the band of 202.71-227.72nm. Although the current measurements of isoprene are mainly GC-MS, PTR-MS and  
253 CIMS methods, the DOAS method has the characteristics of high time resolution, rapid temporal response and simple

254 operation. It is especially suitable for long-term online measurement in the field or forest where the traffic is inconvenient,  
255 and the low cost of instrument is also conducive to build monitoring network.

256

257 Under the condition of zero optical path in the laboratory, several equivalent concentrations were measured by using a series  
258 absorption cell and known concentration of isoprene gas. The correlation coefficient between the measured concentration  
259 and the equivalent concentration was 0.9996, and the slope was 1.065, indicating that the instrument has good linearity and  
260 accuracy. After 23 days of field comparison, there is a good correlation between the results of DOAS and on-line VOCs  
261 instrument, with a correlation coefficient of 0.85 and a slope of 0.86. Considering the differences in measurement principle  
262 and sampled air, the comparison results show a good agreement between these two instruments.

263

264 In order to evaluate the detection limit of DOAS instrument under the actual atmospheric measurement, this study proposes  
265 to calculate the standard deviation of all the data when the measured concentration of isoprene in the ambient air is close to  
266 zero ( $< 0.1$  ppb,  $n = 16387$ ). It is estimated that the detection limit of the DOAS is no more than 0.1 ppb under a  
267 measurement light path of 75 m. Therefore, the DOAS is suitable for long-term monitoring in cities or areas with large  
268 vegetation coverage.

269

270 **Data availability.** Data are published as [https:// DOI: 10.17632/489mvgbsxg.3](https://doi.org/10.17632/489mvgbsxg.3)

271

272 **Author contribution.** The study was designed by SG and BZ. Experiments were performed by YG, RZ and YY. Data  
273 processing and analysis were done by BZ and CG. The paper was written by BZ, SW and SG.

274

275 **Competing interests.** The authors declare that they have no conflict of interest.

276

277 **Acknowledgements.** This research has been supported by the National Key Research and Development Program of China  
278 (grant No. 2017YFC0210002 and 2016YFC0200401), the National Natural Science Foundation of China (grant No.  
279 21777026, 41775113, 21976031, and 42075097).

280

## 281 Reference

- 282 Aydin, Y. M., Yaman, B., Koca, H., Dasdemir, O., Kara, M., Altiok, H., et al. (2014). Biogenic volatile organic compound  
283 (BVOC) emissions from forested areas in Turkey: determination of specific emission rates for thirty-one tree species.  
284 *Science of the Total Environment*, 490, 239-253. <https://doi.org/10.1016/j.scitotenv.2014.04.132>
- 285 Bai, J. (2015). Estimation of the isoprene emission from the Inner Mongolia grassland. *Atmospheric Pollution Research*, 6(3),  
286 406-414. <https://doi.org/10.5094/APR.2015.045>
- 287 Blake, R. S., Monks, P. S., & Ellis, A. M. (2009). Proton-Transfer Reaction Mass Spectrometry. *Chemical Reviews*, 109(3),  
288 861-896. <https://doi.org/10.1021/cr800364q>
- 289 Brauer, C. S., Blake, T. A., Guenther, A. B., Sharpe, S. W., Sams, R. L., & Johnson, T. J. (2014). Quantitative infrared  
290 absorption cross sections of isoprene for atmospheric measurements. *Atmospheric Measurement Techniques*, 7(11),  
291 3839-3847. <https://doi.org/10.5194/amt-7-3839-2014>
- 292 Chen, F. Z., Judge, D. L., Wu, C. Y. R., & Caldwell, J. (1999). Low and room temperature photoabsorption cross sections of  
293  $\text{NH}_3$  in the UV region. *Planetary and Space Science*, 47, 261-266. [https://doi.org/10.1016/S0032-0633\(98\)00074-9](https://doi.org/10.1016/S0032-0633(98)00074-9) Chen,  
294 T., Xue, L., Zheng, P., Zhang, Y., Liu, Y., Sun, J., Han, G., Li, H., Zhang, X., Li, Y., Li, H., Dong, C., Xu, F., Zhang, Q.,  
295 and Wang, W.: Volatile organic compounds and ozone air pollution in an oil production region in northern China, *Atmos.*

296 Chem. Phys., 20, 7069–7086, <https://doi.org/10.5194/acp-20-7069-2020>, 2020.

297 Conor, G. B., Valerio, F., Andrew, D. R., Mohammed, I. M., Mohd, S. M. N., John, A. P., et al. (2020). iDirac: a field-portable  
298 instrument for long-term autonomous measurements of isoprene and selected VOCs. *Atmospheric Measurement*  
299 *Techniques*, 13, 821-838. <https://doi.org/10.5194/amt-13-821-2020>

300 Dawes, A., Pascual, N., Hoffmann, S. V., Jones, N. C., & Mason, N. J. (2017). Vacuum ultraviolet photoabsorption  
301 spectroscopy of crystalline and amorphous benzene. *Physical Chemistry Chemical Physics*, 19, 27544-27555.  
302 <https://doi.org/10.1039/c7cp05319c>

303 EPA, Technical Assistance Document for Sampling and Analysis of Ozone Precursors for the Photochemical Assessment  
304 Monitoring Stations Program, U.S. Environmental Protection Agency, EPA-454/B-19-004 (April, 2009).

305 Eerdeken, G., Ganzeveld, L., Vilà-Guerau de Arellano, J., Klüpfel, T., Sinha, V., Yassaa, N., Williams, J., Harder, H.,  
306 Kubistin, D., Martinez, M., and Lelieveld, J.: Flux estimates of isoprene, methanol and acetone from airborne  
307 PTR-MS measurements over the tropical rainforest during the GABRIEL 2005 campaign, *Atmos. Chem. Phys.*, 9,  
308 4207–4227, <https://doi.org/10.5194/acp-9-4207-2009>, 2009.

309 Gong, D., Wang, H., Zhang, S., Wang, Y., Liu, S. C., Guo, H., Shao, M., He, C., Chen, D., He, L., Zhou, L., Morawska,  
310 L., Zhang, Y., and Wang, B.: Low-level summertime isoprene observed at a forested mountaintop site in southern  
311 China: implications for strong regional atmospheric oxidative capacity, *Atmos. Chem. Phys.*, 18, 14417–14432,  
312 <https://doi.org/10.5194/acp-18-14417-2018>, 2018.

313 HJ 654-2013, Specifications and Test Procedures for Ambient Air Quality Continuous Automated Monitoring System for  
314 SO<sub>2</sub>, NO<sub>2</sub>, O<sub>3</sub> and CO, national standard of China, 2013.  
315 [http://www.cnemc.cn/jcgf/dqhj/201711/t20171108\\_647283.shtml](http://www.cnemc.cn/jcgf/dqhj/201711/t20171108_647283.shtml)

316 Leibrock, E., & Huey, L. G. (2000). Ion chemistry for the detection of isoprene and other volatile organic compounds in  
317 ambient air. *Geophysical Research Letters*, 27(12), 1719-1722. <https://doi.org/10.1029/1999GL010804>

318 Leibrock, E., Huey, L. G., Goldan, P. D., Kuster, W. C., Williams, E., and Fehsenfeld, F. C.: Ground-based  
319 intercomparison of two isoprene measurement techniques, *Atmos. Chem. Phys.*, 3, 67–72,  
320 <https://doi.org/10.5194/acp-3-67-2003>, 2003.

321 Lian, H. Y., Pang, S. F., He, X., Yang, M., Ma, J. B., & Zhang, Y. H. (2020). Heterogeneous reactions of isoprene and ozone  
322 on alpha-Al<sub>2</sub>O<sub>3</sub>: The suppression effect of relative humidity. *Chemosphere*, 240, 124744.  
323 <https://doi.org/10.1016/j.chemosphere.2019.124744>

324 Lu, K., Guo, S., Tan, Z., Wang, H., Shang, D., Liu, Y., Li, X., Wu, Z., Hu, M., and Zhang, Y.: Exploring atmospheric  
325 free-radical chemistry in China: the self-cleansing capacity and the formation of secondary air pollution, *Natl. Sci. Rev.*, 6,  
326 579–594, <https://doi.org/10.1093/nsr/nwy073>, 2018.

327 Martins, G., Ferreira-Rodrigues, A. M., Rodrigues, F. N., de Souza, G. G. B., Mason, N. J., Eden, S., et al. (2009). Valence  
328 shell electronic spectroscopy of isoprene studied by theoretical calculations and by electron scattering, photoelectron, and  
329 absolute photoabsorption measurements. *Physical Chemistry Chemical Physics*, 11, 11219-11231.  
330 <https://doi.org/10.1039/B916620C>

331 Mérienne, M. F., Jenouvrier, A., & Coquart, B. (1995). The NO<sub>2</sub> absorption spectrum. I: Absorption cross-sections at  
332 ambient temperature in the 300-500 nm region. *Journal of Atmospheric Chemistry*, 20(3), 281-297.  
333 <https://doi.org/10.1007/BF00694498>

334 Platt, U., Perner, D., Harris, G.W., Winer, A.M., & Pitts, J.N. (1980). Detection of NO<sub>3</sub> in the polluted troposphere by  
335 differential optical absorption. *Geophysical Research Letters*, 7, 89-92. <https://doi.org/10.1029/GL007i001p00089>

336 Platt, U., Perner, D., & Pätz, H. W. (1979). Simultaneous measurement of atmospheric CH<sub>2</sub>O, O<sub>3</sub>, and NO<sub>2</sub> by differential  
337 optical absorption. *Journal of Geophysical Research: Oceans*, 84(C10), 6329-6335.  
338 <https://doi.org/10.1029/JC084iC10p06329>

339 Platt, U., & Stutz, J. (2008). *Differential Optical Absorption Spectroscopy-Principles and Applications*. Springer.

340 Serralheiro, C., Duflo, D., Ferreira, F. da Silva, Hoffmann, S. V., Jones, N. C., Mason, N. J., et al. (2015). Toluene valence and  
341 Rydberg excitations as studied by ab initio calculations and vacuum ultraviolet (VUV) synchrotron radiation. *The journal*  
342 *of physical chemistry. A*, 119, 9059-9069. <https://doi.org/10.1021/acs.jpca.5b05080>

343 Sindelarova, K., Granier, C., Bouarar, I., Guenther, A., Tilmes, S., Stavrakou, T., et al. (2014). Global data set of biogenic  
344 VOC emissions calculated by the MEGAN model over the last 30 years. *Atmospheric Chemistry and Physics*, 14(17),  
345 9317-9341. <https://doi.org/10.5194/acp-14-9317-2014>

346 Stutz, J. and Platt U., Numerical analysis and estimation of the statistical error of differential optical absorption spectroscopy  
347 measurements with least-squares methods, *Applied Optics*, 35, 6041-6053, 1996.

348 Wu, C. Y. R., Yang, B. W., Chen, F. Z., Judge, D. L., Caldwell, J., & Trafton, L. M. (2000). Measurements of high-, room-, and  
349 low-temperature photoabsorption cross sections of SO<sub>2</sub> in the 2080- to 2950-A region, with application to Io. *Icarus*, 145,  
350 289-296. <https://doi.org/10.1006/icar.1999.6322>

351 Xie, Y., Paulot, F., Carter, W. P. L., Nolte, C. G., Luecken, D. J., Hutzell, W. T., et al. (2013). Understanding the impact of  
352 recent advances in isoprene photooxidation on simulations of regional air quality. *Atmospheric Chemistry and Physics*,  
353 13(16), 8439-8455. <https://doi.org/10.5194/acp-13-8439-2013>

354 Zeng, Y., Shen, Z., Zhang, T., Lu, D., Li, G., Lei, Y., et al. (2018). Optical property variations from a precursor (isoprene) to  
355 its atmospheric oxidation products. *Atmospheric Environment*, 193, 198-204.  
356 <https://doi.org/10.1016/j.atmosenv.2018.09.017>

357 Zhang, X., Huang, T., Zhang, L., Shen, Y., Zhao, Y., Gao, H., et al. (2016). Three-North Shelter Forest Program contribution  
358 to long-term increasing trends of biogenic isoprene emissions in northern China. *Atmospheric Chemistry and Physics*,  
359 16(11), 6949-6960. <https://doi.org/10.5194/acp-16-6949-2016>

360 Zheng, Y., Unger, N., Barkley, M. P., & Yue, X. (2015). Relationships between photosynthesis and formaldehyde as a probe  
361 of isoprene emission. *Atmospheric Chemistry and Physics*, 15(15), 8559-8576. <https://doi.org/10.5194/acp-15-8559-2015>

362 Zhu, J., Wang, S., Wang, H., Jing, S., Lou, S., Saiz-Lopez, A., and Zhou, B.: Observationally constrained modeling of  
363 atmospheric oxidation capacity and photochemical reactivity in Shanghai, China, *Atmos. Chem. Phys.*, 20, 1217–1232,  
364 <https://doi.org/10.5194/acp-20-1217-2020>, 2020.

365